2023 IEEE/ASME International Conference on Advanced Intelligent Mechatronics (AIM)
June 28-30, 2023. Seattle, Washington, USA

Precise Torque Control in High Temperature with Heat Transfer Model based Torque Constant Compensation Algorithm

Jimin Youn[1], Hyeongjun Kim[1], Taeyeon Kim[1] and Kyoungchul Kong[1*]

Abstract— **Robot-driving motors are frequently driven at high temperatures as their weight-to-torque ratio increases for various movements of robots. Such an increase in driving temperature reduces the magnetic flux density of the permanent magnet and the torque constant of the motor. Particularly in applications that mainly utilize feed-forward torque control without an additional torque sensor, this torque constant reduction leads to severe degradation of torque control performance. This research proposes a torque control method that compensates for the torque constant depending on temperature by identifying the relationship between magnet temperature and the torque constant. In addition, since it is difficult to measure the temperature of the rotor-attached magnet directly, lumped parameter thermal network(LPTN) and full-state observer are used for magnet temperature estimation. The robustness of the proposed controller is verified through experimental results of torque error from 6.19% without compensation to 0.65% with compensation.**

I. INTRODUCTION

In areas where complex mobility is required, such as humanoids, quadrupedal walking robots, and wearable robots, the mobility and weight of the system are directly related. For complicated movements, various methods to maximize output torque in set weight limits are introduced. There are some studies to obtain control performance with slight energy loss by lowering the deceleration ratio and increasing the deceleration efficiency with high allowable current [1]. Other methods include motor design with distinct materials, such as permanent magnets with exceptional molecular arrangements or utilizing halbach arrays [2], [3]. As a result, power efficiency relative to the average weight of the robot system is gradually increasing. Therefore, it is a trend to pass current through the motor beyond its recommended usage standard.

However, as a high current pass through BLDC motors, the internal temperature rises due to Joule heat and eddy current. Then, the arrangement of magnet-constituting-atoms within the permanent magnet is disrupted, decreasing the magnetic flux density of the magnet and the torque constant of the motor [4]. When the magnet is heated by $100°C$, the output torque decreases from 10% to 20% depending on the material of the magnet [5]. This means the increased internal temperature of the motor acts as a complex cause of error in torque control performance. Control performance can be maintained by using torque sensors, but there are many difficulties in attaching additional sensors, especially in the wearable robot field. Wearable robots have substantial limitations, particularly on their weight, since they are directly related to human burden [6]. In addition, there is a strict standard for control performance according to their high priority of safety, and stability [7]. In other words, the driving system of wearable robots should be able to compensate for the influence of high temperatures without attaching a bulky torque sensor.

Moreover, as output torque change is attributed to the temperature of a rotor-attached permanent magnet, several methodologies for estimating the magnet temperature have been proposed. Finite element method(FEM) can estimate temperatures accurately, but this method is not suitable for robot applications that require real-time control due to its large computational volume [8], [9]. Several estimation methods can be implemented in real-time [10], and one is temperature estimation based on flux observer [11]–[13]. However, this method can only be used in high-speed applications where magnetic flux changes are prominent. An invasive method of obtaining temperature-dependent flux variation by measuring current response has also been proposed [14], [15]. This method can be implemented for low-speed driving, but it can only be used in thermal and electrical steady states. Another solution is to identify the lumped parameter thermal network(LPTN), an equivalent system that simplifies the heat transfer of the actual system [16]–[18]. Although the abstraction level is higher than other methods, it is suitable for applications with dynamic movements and wide-range speeds, such as wearable robots.

However, it is difficult to find a study that supplements the torque control performance considering the change in magnetic flux density. This paper introduces mathematical modeling of magnetic flux density change according to magnet temperature using LPTN methodology. In addition, an algorithm that improves the feed-forward torque control performance by compensating for torque constant change is proposed.

The contribution of this study is as follows: 1) The torque constant according to magnet temperature was modeled, and a temperature-robust torque controller was designed based on the model. 2) The magnet temperature, a direct cause of torque constant change, is accurately estimated through a thermal model and full-state observer.

*This work was supported in part by National Research Foundation of Korea grant(NRF) funded by the Korean government (Grant 2022R1A3B107788011), in part by Robot Industrial Technology Development Project (20018157) funded by the Korean government(MOTIE)

[1]J. Youn, H. Kim, T. Kim and K. Kong are with the Department of Mechanical Engineering, Korea Advanced Institute of Science and Technology (KAIST), Daejeon, Korea yjm7845@kaist.ac.kr, khj970311@kaist.ac.kr, ty.kim@kaist.ac.kr and kckong@kaist.ac.kr

978-1-6654-7633-1/23/$31.00 ©2023 IEEE

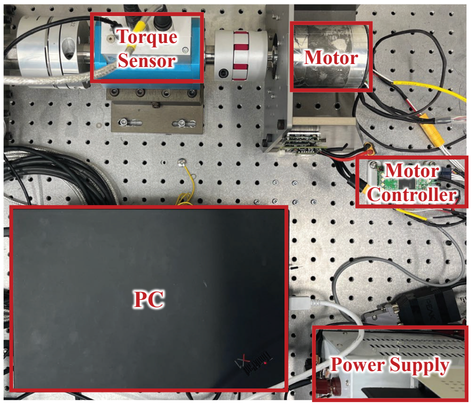

Fig. 1. Experimental setup.

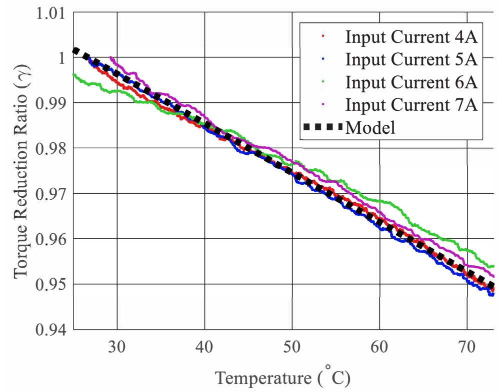

Fig. 2. Identified torque constant - temperature relation.

II. TORQUE CONSTANT - TEMPERATURE RELATION IDENTIFICATION

This research proposes a feed-forward torque controller that is robust to temperature by identifying torque constant in magnet temperature. To this end, the relationship between these two is experimentally identified in an experimental setting, as shown in Fig. 1. In this experiment, the temperature of the permanent magnet and generated torque are measured when a constant current flows through the motor. The output terminal of the motor was fixed during the experiment to measure the rotor temperature where a permanent magnet is attached. Allied Motion's HT02305 motor is used during the experiment, and the self-developed Bumblebee motor driver is used for current control. TMP36 temperature sensor from Analog Devices, and 4503B torque sensor from Kistler are used for temperature and torque measurement, respectively. Each data is measured with a sampling frequency of 10Hz, and torque constant is obtained based on the measured torque values while 4A, 5A, 6A, and 7A current control. In order to find the tendency of torque change to temperature, the torque constant reduction ratio γ is identified. Since the relation between torque constant and temperature is considered first-order generally [5], the results are fitted in the first-order equation through MATLAB cure-fitting tool. The relation is identified as

$$\gamma(T_R) = \frac{K_t(T_R)}{K_t(25°C)} = -0.00109 \cdot T_R + 1.03, \quad (1)$$

where $K_t(25°C)$ is the torque constant at room temperature and measured as $0.3355Nm/A$; γ is the torque constant reduction ratio; T_R is rotor temperature. As in Fig. 2, modeled torque constant shows an error of up to 0.5621% and 0.2998% on average compared to the measured torque constant. In addition, the torque constant decreased by 5.74% on average at $75°C$ than that of room temperature. This means that when the torque constant is fixed at room temperature, a torque constant error of 5.74% occurs at $75°C$. The validity of identified relation is proved in that this error is reduced to a maximum of 0.56% and an average of 0.30% through the proposed model.

III. THERMAL MODEL OF BLDC MOTOR

A. Lumped Parameter Thermal Network Model

The permanent magnet temperature must be accurately measured to compensate for a decrease in torque output according to temperature. However, since magnet attached rotor rotates rapidly as the motor is driven, it is impossible to measure the magnet temperature using a contact-type temperature sensor. Among non-contact-type sensors, it is possible to measure the rotor temperature using a small infrared temperature sensor. Still, infrared sensors are not suitable for temperature measurements that require both real-time and accuracy since the response is slow, and their accuracy highly depends on the emissivity of the measured object [19]. Therefore, a method of accurate estimation is required for torque constant compensation. In this paper, the LPTN of the motor is set and used to estimate the permanent magnet temperature in real-time accurately.

B. Proposed Thermal Model

In the design of LPTN, as the number of considered nodes increases, the estimation accuracy increases, as well as computation time and complexity. However, if the characteristics of the motor are well considered, relative accuracy can be ensured even with the small number of nodes. Therefore, selecting an appropriate model for accuracy and real-time estimation is essential. As shown in Fig. 3, the motor stator, rotor, and housing are selected as nodes of the proposed heat transfer model. The stator node includes a stator core and stator winding. Two are considered one node since heat conduction between them is accessible with a wide contact area. The rotor node includes a rotor core, permanent magnet, and rotating shaft. The end cap and casing are considered as one housing node, although the thermal distance between the two is relatively long. This is because the material constituting the housing node is aluminum, of which the thermal conductivity is more than three times that of iron and four times that of carbon steel [20].

The heat transfer proposed in Fig. 3(a) can be expressed as LPTN, as in Fig. 3(b). Here, T_S, T_R, T_H, and T_A represent stator, rotor, housing, and ambient temperature, respectively; R_{SR}, R_{SH}, R_{RH}, R_{HA} represent the thermal resistance between

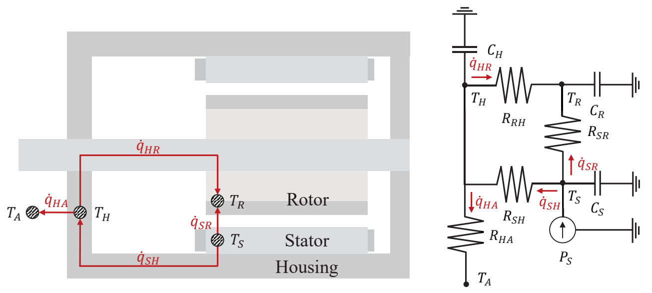

(a) (b)

Fig. 3. Proposed thermal model. (a) Modeled heat flow. (b) Proposed thermal network.

stator and rotor, stator and housing, rotor and housing and housing and ambient, respectively; C_S, C_R, and C_H represent the thermal capacity of the stator, rotor, and housing, respectively; P_S represents the loss of stator.

C. State-Space Representation of Proposed Thermal Model

The heat transfer equation of the proposed LPTN can be expressed in a discrete-time state-space equation as

$$\begin{bmatrix} T_S(k+1) \\ T_R(k+1) \\ T_H(k+1) \end{bmatrix} = F \begin{bmatrix} T_S(k) \\ T_R(k) \\ T_H(k) \end{bmatrix} + G \begin{bmatrix} i^2(k) \\ T_A(k) \end{bmatrix}, \quad (2)$$

where i and R are the current through winding and terminal resistance of winding, respectively. Here, the state matrix, $F \in \mathbb{R}^{3\times3}$ and input matrix, $G \in \mathbb{R}^{3\times2}$ are to be identified in the next section.

D. Thermal Model Identification

The Least squares method is used to identify the state matrix and input matrix of the proposed model. An experiment is conducted while the motor shaft is fixed since the temperature of all nodes, including rotor temperature, should be measured. Here, it is assumed that convection heat transfer due to rotation is insignificant. Therefore, the model can be identified in a fixed state. The experimental setup is as in Fig. 1, and the same types of equipment are used as in Section II. While the current is controlled as 5A, 6A, and 7A, the stator, rotor, and housing temperatures are measured until the stator temperature rises to 95°C. This experiment is repeated four times, respectively. Then, the state matrix and input matrix are identified by applying the least squares method to the measured temperature data. Based on the identified model, the temperature of the permanent magnet is estimated for sinusoidal input currents with RMS magnitude of 5A, 6A, 7A. Table I shows the RMS errors of temperature estimation. The estimation accuracy is as low as 4.0°C, in average, meaning that identified model has some error itself. Here, the ambient temperature, T_A, is assumed constant as 25°C.

IV. REAL-TIME ROTOR TEMPERATURE ESTIMATION BASED ON HEAT TRANSFER MODEL

A. Design and Implementation of Full-State Observer

The permanent magnet temperature is estimated in real time based on the identified heat transfer model. In the model verification of Section III. *D*, a non-negligible error existed with the sinusoidal current input, meaning that error exists in the proposed LPTN model. In order to increase the estimation accuracy, the stator temperature is measured in real-time through a temperature sensor. The measurement improved the estimation accuracy by compensating for model error through the designed full-state observer.

B. Verification of Temperature Estimation

The magnet temperature estimation using the identified model and observer is verified with real-time magnet temperature estimation. The verification included estimation with sinusoidal current, which validates periodicity, commonly generated in robot control. The RMS magnitude of sinusoidal current is controlled as 4A, 5A, 6A, and 7A. Here, the input is controlled with 0.1Hz frequency. During verification, measured temperature is implemented through a discrete-time low pass filter of 0.02Hz, and such frequency is designed considering the time constant of the heat transfer model. Table II shows the RMS error of these temperature estimations. Also, Fig. 4 represents the estimation error with and without state observer to sinusoidal input current. Table III shows the performances of these estimations using RMS errors. As a result of verification, the RMS error of estimation is lowered as 40% by implementing a state observer. With the observer, the robustness of temperature estimation to time-varying current input is reinforced. In brief, the estimation accuracy is augmented by supplementing a model error through a state observer.

V. DESIGN AND IMPLEMENTATION OF TORQUE CONSTANT COMPENSATOR

A. Design of Torque Constant Compensator

A torque constant compensator is implemented for robust torque control for temperature. Fig. 5 shows the block diagram of the entire closed-loop system, including the proposed controller. Here, τ_d, i_d, and u_c represent torque reference, current reference, and control input, respectively; τ and i represent output torque and output current, respectively. Torque compensation controller can be designed using

TABLE I

RMS ERROR OF TEMPERATURE ESTIMATION.

The magnitude of current [A]	RMS error with sinusoidal current [$\circ C$]
5	4.8636
6	4.5921
7	2.4782

TABLE II
RMS ERROR OF TEMPERATURE ESTIMATION WITH STATE OBSERVER.

The magnitude of current [A]	RMS error with sinusoidal current [$\circ C$]
4	2.0004
5	1.9662
6	1.2281
7	1.1717

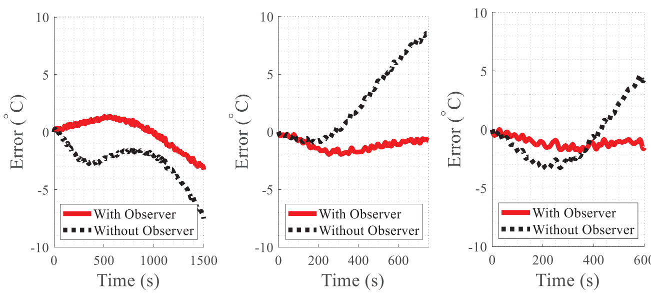

(a) (b) (c)

Fig. 4. Error of temperature estimation with and without observer while sinusoidal current control. (a) With 5A input current. (b) With 6A input current. (c) With 7A input current.

TABLE III
COMPARE OF ESTIMATION ERROR WITH AND WITHOUT OBSERVER.

Implementation of state observer	RMS error with sinusoidal current [$\circ C$]
Not implemented	3.9780
Implemented	1.5916

identified torque constant reduction ratio in (1) as

$$C(T_R) = \gamma(T_R)^{-1} \simeq 0.00122 \cdot T_R + 0.9646. \quad (3)$$

By substituting the estimated rotor temperature for (3), the current reference is determined as

$$u_c(k) = i_d(k)C(\hat{T}_R(k)). \quad (4)$$

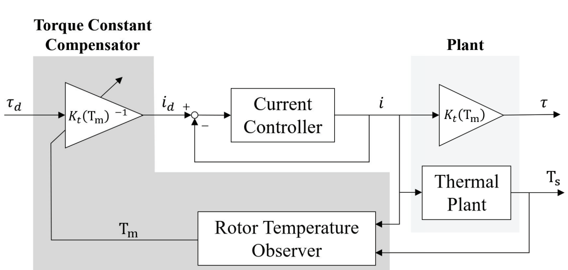

Fig. 5. The block diagram of proposed controller.

B. Experimental Results

Fig. 6 shows the torque control performance according to increasing rotor temperature with and without a torque constant compensator. When the RMS magnitude of 4A,

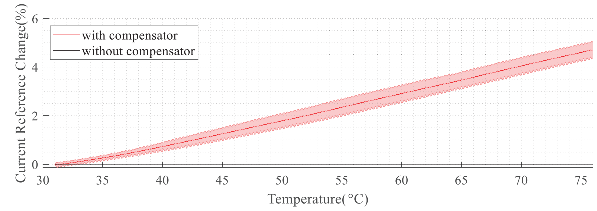

(a)

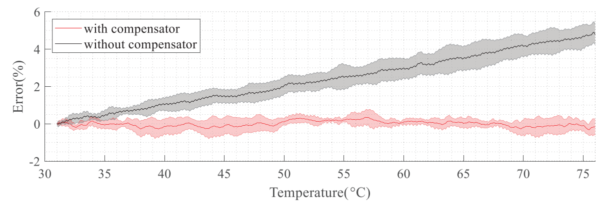

(b)

Fig. 6. Performance evaluation of proposed torque constant compensator. (a) Change of control input respect to temperature. (b) Error to torque reference respect to temperature.

5A, 6A, and 7A sinusoidal currents are applied, output torque linearly decreases until 6.19% without a compensator, on average. However, with the proposed controller, torque decrease hardly exists as 0.65% even at the highest temperature, on average. This means that the proposed controller can robustly control torque despite the magnet temperature changes.

VI. CONCLUSION

In general, the control performance of feed-forward torque controllers, widely used in the wearable robot field, significantly decreases as the permanent magnet temperature of the motor increases. This research proposed a torque control algorithm that compensates torque constant in real-time, based on the identified relationship between magnet temperature and torque constant. The magnet's temperature while rotating is estimated using LPTN which is identified by the least squares method. By using a full-state observer that uses an additional temperature sensor, the estimation accuracy is improved and verified with multiple experiments. The robustness of torque constant estimation that varies to temperature is verified for sinusoidal and stall current input with various magnitudes.

For future studies, the control performance in practice should be verified while the motor rotates at high speed. The experiments in this research are done with attachable temperature sensors in static conditions. With available non-attach temperature measurement devices for identifying LPTN, the advanced full-state temperature observer that can consider the rotation speed should be developed. Furthermore, the condition under which the motor is driven within a safe temperature range should be found mathematically.

References

[1] P. M. Wensing, A. Wang, S. Seok, D. Otten, J. Lang, and S. Kim, "Proprioceptive actuator design in the mit cheetah: Impact mitigation and high-bandwidth physical interaction for dynamic legged robots," *IEEE Transactions on Robotics*, vol. 33, no. 3, pp. 509–522, 2017.

[2] H. Chang, S. J. Kim, and J. Kim, "Feedforward motion control with a variable stiffness actuator inspired by muscle cross-bridge kinematics," *IEEE Transactions on Robotics*, vol. 35, no. 3, pp. 747–760, 2019.

[3] Y. Wei, V. H. Nguyen, and W.-J. Kim, "A 3-d printed halbach-cylinder motor with self-position sensing for precision motions," *IEEE/ASME Transactions on Mechatronics*, vol. 27, no. 3, pp. 1489–1497, 2022.

[4] J. Schützhold and W. Hofmann, "Analysis of the temperature dependence of losses in electrical machines," in *Proc. of the 2013 IEEE Energy Conversion Congress and Exposition*, 2013, pp. 3159–3165.

[5] M. Sidahmed and M. Mahmoud, "Effect of plant parameter variation on feedback control loop(dc motor temperature effect model)," *International Journal of Advance Research in Computer Science and Management Studies*, vol. 2, pp. 384–388, 2014.

[6] H. Choi, B. Na, S. Kim, J. Lee, H. Kim, D. Kim, D. Cho, J. Kim, S. Shin, D.-W. Rha, and K. Kong, "Angel-suit: a modularized lower-limb wearable robot for assistance of people with partially impaired walking ability," in *Proc. of the 2019 Wearable Robotics Association Conference (WearRAcon)*, 2019, pp. 51–56.

[7] T. Zhang and H. Huang, "Design and control of a series elastic actuator with clutch for hip exoskeleton for precise assistive magnitude and timing control and improved mechanical safety," *IEEE/ASME Transactions on Mechatronics*, vol. 24, no. 5, pp. 2215–2226, 2019.

[8] H.-K. Yeo, H.-J. Park, J.-M. Seo, S.-Y. Jung, J.-S. Ro, and H.-K. Jung, "Electromagnetic and thermal analysis of a surface-mounted permanent-magnet motor with overhang structure," *IEEE Transactions on Magnetics*, vol. 53, no. 6, pp. 1–4, 2017.

[9] P. Zhao and Y. Yu, "Analysis of influence of permanent magnet demagnetization on motor temperature rise," vol. 2395, no. 1, p. 012022, 2022.

[10] O. Wallscheid, T. Huber, W. Peters, and J. Böcker, "Real-time capable methods to determine the magnet temperature of permanent magnet synchronous motors — a review," in *Proc. of the IECON 2014 - 40th Annual Conference of the IEEE Industrial Electronics Society*, 2014, pp. 811–818.

[11] X. Xiao, C. Chen, and M. Zhang, "Dynamic permanent magnet flux estimation of permanent magnet synchronous machines," *IEEE Transactions on Applied Superconductivity*, vol. 20, no. 3, pp. 1085–1088, 2010.

[12] A. Specht and J. Böcker, "Observer for the rotor temperature of ipmsm," in *Proc. of the Proceedings of 14th International Power Electronics and Motion Control Conference EPE-PEMC 2010*, 2010, pp. T4–12–T4–15.

[13] A. Specht, O. Wallscheid, and J. Böcker, "Determination of rotor temperature for an interior permanent magnet synchronous machine using a precise flux observer," in *Proc. of the 2014 International Power Electronics Conference (IPEC-Hiroshima 2014 - ECCE ASIA)*, 2014, pp. 1501–1507.

[14] M. Ganchev, C. Kral, H. Oberguggenberger, and T. Wolbank, "Sensorless rotor temperature estimation of permanent magnet synchronous motor," in *Proc. of the IECON 2011 - 37th Annual Conference of the IEEE Industrial Electronics Society*, 2011, pp. 2018–2023.

[15] M. Ganchev, C. Kral, and T. Wolbank, "Hardware and software implementation of sensorless rotor temperature estimation technique for permanent magnet synchronous motor," in *Proc. of the 2012 Electrical Systems for Aircraft, Railway and Ship Propulsion*, 2012, pp. 1–6.

[16] G. D. Demetriades, H. Z. de la Parra, E. Andersson, and H. Olsson, "A real-time thermal model of a permanent-magnet synchronous motor," *IEEE Transactions on Power Electronics*, vol. 25, no. 2, pp. 463–474, 2010.

[17] T. Huber, W. Peters, and J. Böcker, "A low-order thermal model for monitoring critical temperatures in permanent magnet synchronous motors," in *Proc. of the 7th IET International Conference on Power Electronics, Machines and Drives (PEMD 2014)*, 2014, pp. 1–6.

[18] G. Dajaku and D. Gerling, "An improved lumped parameter thermal model for electrical machines," in *Proc. of the 17th International conference on electrical machines (ICEM2006)*. Citeseer, 2006, pp. 1–6.

[19] D. D. Reigosa, F. Briz, P. García, J. M. Guerrero, and M. W. Degner, "Magnet temperature estimation in surface pm machines using high-frequency signal injection," *IEEE Transactions on Industry Applications*, vol. 46, no. 4, pp. 1468–1475, 2010.

[20] J. Carvill, *Mechanical engineer's data handbook*. Butterworth-Heinemann, 1994.